

## First Results from MASIV: The Micro-Arcsecond Scintillation-Induced Variability Survey

J. E. J. Lovell<sup>1</sup>

Jim.Lovell@csiro.au

D. L. Jauncey<sup>1</sup>

David.Jauncey@csiro.au

H. E. Bignall<sup>2,1,3</sup>

bignall@jive.nl

L. Kedziora-Chudczer<sup>1</sup>

Lucyna.Kedziora-Chudczer@csiro.au

J-P. Macquart<sup>4</sup>

jpm@astro.rug.nl

B. J. Rickett<sup>5</sup>

rickett@ece.ucsd.edu

A. K. Tzioumis<sup>1</sup>

Tasso.Tzioumis@csiro.au

### ABSTRACT

We are undertaking a large-scale, Micro-Arcsecond Scintillation-Induced Variability (MASIV) survey of the northern sky,  $\delta > 0^\circ$ , at 4.9 GHz with the VLA. Our objective is to construct a sample of 100 to 150 scintillating extragalactic sources with which to examine both the microarcsecond structure and the parent populations of these sources, and to probe the turbulent interstellar medium responsible for the scintillation. We report on our first epoch of observations which revealed variability on timescales ranging from hours to days in 85 of 710 compact flat-spectrum sources. The number

---

<sup>1</sup>Australia Telescope National Facility, CSIRO, PO Box 76, Epping, NSW 1710, Australia

<sup>2</sup>Department of Physics and Mathematical Physics, University of Adelaide, SA 5005, Australia

<sup>3</sup>now at Joint Institute for VLBI in Europe, Postbus 2, 7990 AA, Dwingeloo, The Netherlands

<sup>4</sup>Kapteyn Astronomical Institute, University of Groningen, Postbus 800 9700 AV, Groningen, The Netherlands

<sup>5</sup>University of California San Diego, La Jolla, CA 92093

of highly variable sources, those with RMS flux density variations greater than 4% of the mean, increases with decreasing source flux density but rapid, large amplitude variables such as J1819+3845 are very rare. When compared with a model for the scintillation due to irregularities in a 500 pc thick electron layer, our preliminary results indicate maximum brightness temperatures  $\sim 10^{12}$  K, similar to those obtained from VLBI surveys even though interstellar scintillation is not subject to the same angular resolution limit.

*Subject headings:* galaxies: active — ISM: structure — radio continuum

## 1. Introduction

Considerable evidence has now accumulated to demonstrate that interstellar scintillation (ISS) in the turbulent interstellar medium (ISM) of our Galaxy, is the principal mechanism responsible for the intra-day variability (IDV) seen in many flat-spectrum Active Galactic Nuclei at centimeter wavelengths. Much of this evidence has come from observations of the three fastest known IDV sources, B0405–385 (Kedziora-Chudczer et al. 1997), B1257–326 (Bignall et al. 2003) and J1819+3845 (Dennett-Thorpe & de Bruyn 2000). The rapid variability in these sources makes possible the detection and measurement of any pattern delay at widely spaced radio telescopes, as might be expected if ISS is the cause of the IDV.

Such a pattern time delay was first measured in B0405–385 between the ATCA and the VLA at 5 GHz (Jauncey et al. 2000) despite the unfavorable geometry for this measurement for such a southern source. This was soon followed by similar measurements with J1819+3845 (Dennett-Thorpe & de Bruyn 2002), where the high northern declination of the source and the northern location of both the VLA and the WSRT made this a very elegant experiment. Most recently, a pattern time delay has also been measured in B1257–326 between the ATCA and the VLA at 4.9 and 8.5 GHz (Bignall 2003; Jauncey et al. 2003; Bignall et al., in preparation).

The presence of such a pattern time delay implies that the turbulent structures in the ISM are moving at a speed close to the  $30 \text{ km s}^{-1}$  orbital speed of the Earth. For part of the year the Earth and the ISM move together, the relative speed is low and the scintillation pattern moves across the observer slowly. Six months later the Earth moves in the opposite direction so the relative speed is high and the scintillation pattern moves more rapidly.

Such an “annual cycle” has now been reported in three sources, J1819+3845 (Dennett-Thorpe & de Bruyn 2001), B0917+624 (Rickett et al. 2001; Jauncey & Macquart 2001) and B1257-326 (Bignall et al. 2003), and evidence is accumulating for its presence in several more sources. Moreover, an annual cycle has been detected in B1257–326 not only in the characteristic time scale,  $T_{\text{char}}$ , but also in the time delay between the scintillation patterns at 8.6 and 4.8 GHz. Bignall et al (2003) suggest that this may be due to an offset between the central components of the source

at each frequency, as might be expected if the source were jet-like on a microarcsecond scale, and optically thick between 4.8 and 8.6 GHz. This second annual cycle occurs as the ISM passes first across the 8.6 GHz then across the 4.8 GHz component, with the apparent displacement on the sky due to the displacement of the  $\tau = 1$  surfaces along the jet. If the position of the surfaces scales as  $\nu^{-1}$  along the jet (Blandford & Konigl 1979), this implies a displacement of 0.1 pc (Bignall et al. 2003).

The above observations establish unequivocally ISS in the local Galaxy as the principal cause of the IDV seen in these sources. Moreover, the long time for which IDV has been seen in some of these sources, more than a decade for B0917+624 (Fuhrmann et al. 2002) and more than 5 years for both B1257-326 and J1819+3845, suggests that such scintillating components are relatively long lived despite their small physical sizes.

A source must be small in order to scintillate. In the weak scattering case, most commonly encountered at frequencies  $\gtrsim 5$  GHz, the source angular size,  $\theta_S$ , must be comparable to the angular size of the first Fresnel zone (e.g. Narayan 1992). This implies an angular size

$$\theta_S \lesssim \sqrt{\lambda/2\pi D}$$

which is at most tens of microarcseconds for screen distances,  $D$ , of tens to hundreds of parsecs.

The limiting angular size for scintillation varies inversely with the square root of the screen distance, and thus the brightness temperatures inferred from ISS scale with the screen distance. Reliable screen distances and thus brightness temperatures have been estimated for five scintillators. Rickett et al. (1995) found  $6 \times 10^{12}$  K for B0917+624 for scattering at 200 pc. For the three fast scintillators, B0405–385, B1257–326 and J1819+3845, recent careful analyses has found very nearby screens with typical distances of 10 to 30 pc (Rickett, Kedziora-Chudczer & Jauncey 2002; Bignall et al. 2003; Dennett-Thorpe & de Bruyn 2000). Such nearby screens yield brightness temperatures of  $2 \times 10^{13}$  K,  $4 \times 10^{12}$  K and  $5 \times 10^{12}$  K respectively. For B1519–273 a lower limit to the screen distance of 390 pc has been found, based on the measured 1.6 GHz angular size limit. This yields a brightness temperature lower limit of  $5 \times 10^{13}$  K, or possibly as high as  $6 \times 10^{14}$  K (Macquart et al. 2000). These results imply large Doppler factors for these sources, at least as high as several hundred (Readhead 1994), significantly higher than those seen in existing VLBI surveys (Kellermann et al. 2000; Marscher et al. 2000).

## 2. The need for a large survey

The realization that ISS is the principal physical process responsible for IDV at centimetre wavelengths suggests that a large-scale scintillation survey may address many questions regarding both source microarcsecond structures and properties of the ISM not otherwise accessible. To date, IDV surveys have been relatively small, restricted to of order 100 of the strongest flat-spectrum sources (Heeschen 1984; Quirrenbach et al. 1989; Kedziora-Chudczer et al. 2001). These surveys

have shown that up to  $\sim 20\%$  of the strong sources scintillate, but the small size of these surveys has yielded samples of no more than 20 scintillators, insufficient for reliable statistical investigations.

Therefore we have undertaken a large scale 4.9 GHz Micro-Arcsecond Scintillation-Induced Variability (MASIV) survey with the VLA. The aim is to construct a large, statistically significant sample of 100 to 150 scintillating sources. 4.9 GHz was chosen as the observing frequency as it is in the weak scattering regime where the variations are rapid, but is close to the transition frequency where the largest amplitude scintillations and shortest timescales are seen over most of the sky (Walker 1998).

In order to understand the sources themselves, it is also necessary to understand the effects of the ISM, since the two are intimately linked via the scintillation process. Assuming that the extragalactic sources are distributed uniformly over the sky, the observed distribution of 100 or more scintillators may shed light on the distribution of scattering material throughout the northern Galaxy. In particular, the presence of new fast scintillators can reveal the presence of nearby scattering material. Furthermore, determination of the annual cycle distribution will lead to the overall distribution of the velocity of the ISM.

For the sources themselves, the survey results lead directly to an understanding of the dependence on scintillation on flux density, spectral index, the nature of optical counterpart, redshift, luminosity, milliarcsecond structure and evolution. Most importantly, the survey allows us to better characterize the scattering process responsible and hence constrain the source brightness temperatures.

To make sure that the survey is unbiased with regard to characteristic scintillation time scales, all sources were observed over three well-spaced epochs during our observations, so that sources in the “slow” part of their annual cycle would not be missed. Three well-spaced epochs also allows us to better find those sources like B0405–385 whose scintillation outbursts are episodic (Kedziora-Chudczer et al. 1997). Each session extended over three or more days to prevent missing the slower scintillators. Moreover, the 2 hour minimum observing interval gave sufficient coverage each day to reliably recognize any variability.

We expect that any new fast scintillators found in the survey will reveal the presence of nearby regions of interstellar turbulence in the Galaxy. Both of the long-lived fast scintillators are among the weakest known, so the survey included a selection of both strong,  $\sim 1$  Jy, and weak,  $\sim 0.1$  Jy, sources. Moreover, as the VLA was in a variety of configurations during the year, we selected only sources that would appear point-like to the VLA at all resolutions. We selected compact flat-spectrum sources as they are expected to possess a compact nucleus. The sources were selected from the JVAS (Patnaik, Browne, Wilkinson, & Wrobel 1992; Browne, Wilkinson, Patnaik, & Wrobel 1998; Wilkinson et al. 1998) and CLASS (Myers et al. 1995) catalogs of sources unresolved at 8.5 GHz with the VLA. From the JVAS catalog we selected all sources with greater than 95% of their flux density in an unresolved component and from the CLASS survey we selected all sources with modeled source sizes less than 50 mas. Sources were rejected if the catalogs indicated the

presence of confusing sources in the field. We cross-correlated these sources with the NVSS catalog to obtain spectral indices of all sources and thus a flat-spectrum sample. We chose a spectral-index lower-limit of  $-0.3$  ( $S \propto \nu^\alpha$ ) which provided a sample of 1871 sources stronger than 100 mJy at 8.5 GHz.

To reduce this to a manageable quantity for  $\sim 2$  hourly flux density monitoring, the sample was further reduced into strong and weak sub-samples of approximately 300 sources each. The weak sample consists of sources with 8.5 GHz flux densities between 105 and 130 mJy and the strong sample contains sources stronger than 600 mJy. We also selected a sub-sample of sources between 130 and 600 mJy with  $4.5 \text{ h} \leq \text{RA} < 7.5 \text{ h}$  or  $16.5 \text{ h} \leq \text{RA} < 19.5 \text{ h}$  and  $\delta \geq 35^\circ$ . These two “windows” coincide with regions of the sky where the predicted ratio between the fastest and slowest variability timescale over the course of a year are at their minimum ( $\text{RA} \approx 6 \text{ h}$ ) and maximum ( $\text{RA} \approx 18 \text{ h}$ ) for ISS-induced variability in a plasma moving with the LSR (Rickett 2002), and thus let us probe a full range of flux densities for these two regions. The declination limit was chosen to avoid excessive azimuth slew times at the VLA for sources near transit. The total number of sources in our sample is 710.

### 3. Observations

Our first epoch of observations spanned 72 hours from 2002 January 19 to 2002 January 22 during reconfiguration from D to A array. At the start of our observations all antennas had been moved into A-array except for two on the south spur of the array, separated by 40 m. The observations were conducted in a five-subarray mode. The combined strong and weak samples were divided into four declination bands and one subarray was assigned to each. The fifth subarray was assigned to the intermediate flux-density sources in the minimum and maximum annual modulation ratio windows defined above.

Each subarray was scheduled so that every source was observed for one minute every  $\sim 2$  h while it was above an elevation of  $15^\circ$ . Antennas were assigned to subarrays to form long baselines to reduce possible contributions from any extended structure. Shadowing was avoided for the two antennas in D-array by assigning the northern-most antenna to the northern-most declination band and the southern-most to the southern declination band. For flux density calibration, each subarray observed B1328+307 (3C286) and J2355+4950 every  $\sim 2$  hours. B1328+307 is the primary flux density calibrator for the VLA and J2355+4950 is a GPS source, not likely to vary over short timescales, and is monitored regularly at the VLA as part of a calibrator monitoring program.

The data from our observations were loaded into AIPS in real-time using the on-line FILLM task, thus providing quick access to the data. After the first 24 h we performed a rudimentary amplitude calibration and began searching for evidence of short timescale variability with peak-to-peak amplitudes greater than  $\sim 10\%$ , well above our estimated systematic errors of a few percent. Once these sources were identified we scheduled additional scans on them in the last 24 h of our

observations to improve the sampling and hence our estimation of the variability timescale.

Following the observations we applied a more rigorous calibration of both total intensity and linear polarization data. This required particular care as many antennas had recently been moved and their pointing calibration observations were not complete. The residual pointing errors may depend on azimuth and elevation so we chose several bright, non-variable sources in each subarray at a range of right ascensions as gain calibrators for surrounding sources. Precautions were taken to ensure that the calibrators themselves were not variable: if a given calibrator caused the majority of sources against which it was applied to vary, then another calibrator was chosen.

As the subarray beam pattern rotates on the sky, the presence of arcsecond scale structure adds alternatively in-phase and out-of-phase with the central unresolved “core” creating the appearance of variability. However, it then has the same variability character on each of the three days observations, and such a repetitive pattern is relatively easily seen in the data. Moreover, imaging the three day data set quickly resolves any ambiguities. Snapshot images were therefore made of each source showing evidence of variability to guard against such spurious detection of IDV. This is most important when the VLA was in its more compact configurations.

#### 4. Results

In order to separate variable from non-variable sources it is essential to determine reliably the uncertainties in the VLA flux density measurements. As a first step we plotted, in Figure 1, the modulation index (RMS divided by the mean flux density), versus mean flux density, for each of the 710 sources in the survey. Figure 1 shows clearly the flux density groupings of the strong and weak samples, and that the great majority of the sources have average RMS errors well below 5%.

Uncertainties in flux density measurements are made up of two components, one,  $s$  Jy, due to noise and confusion, that is independent of flux density, and the other,  $p$  %, that is proportional to flux density and due primarily to pointing offsets. The dominant uncertainty among the strong sources is  $p$  while  $s$  is the main contributor among weak sources. Examination of Figure 1 indicates that  $s$  is close to 1.5 mJy and  $p$  is close to 1%. As a first step, we then selected for a more detailed examination, those sources with

$$\text{RMS} \geq \sqrt{(2s)^2 + \left(\bar{S} \frac{2p}{100}\right)^2} \text{ Jy}$$

where  $\bar{S}$  is the mean flux density at 4.9 GHz. This corresponds to a simple  $\chi$ -squared test to identify those sources whose scatter is well in excess of the overall population errors; that is those that are likely variables. This procedure identified 99 sources. While this is not the most effective way of finding the variable sources, it serves as an effective starting point to determine the errors for the survey as a whole.

Data collected for each of these 99 sources were then examined in detail. In many instances not only were there obvious strong flux density changes, but the pattern of the variations are remarkably similar to those seen in many of the known IDV sources (Kedziora-Chudczer et al. 2001). To give a flavor of the range of variations seen, and to provide an initial catalog of sources from which others may wish to conduct more detailed investigations, we list in Table 1 all sources with a mean flux density greater than 100 mJy and modulation indices of 0.04 or more, making a total of 29 sources. Light curves for these sources are also shown in Figures 2-5 and we now discuss these sources individually from the shortest to the longest variability timescales.

Variability was detected on a full range of timescales from less than two hours to greater than three days. (We define timescale here as the mean time between a peak and a minimum in a light-curve). In Figure 2 we show two of the most rapid variables detected: J0929+5013 and J1819+3845. Both are clearly under-sampled in our survey observations but are detected as variable nonetheless.

J0929+5013 is a BL Lac object (Nass et al. 1996). Like most strong ( $S_{4.9\text{GHz}} > 0.3$  Jy) sources listed in Table 1, it has been observed at milliarcsecond-scale resolution and is compact (Beasley et al. 2002).

J1819+3845 was serendipitously discovered to be an IDV 3 years ago (Dennett-Thorpe & de Bruyn 2000), and exhibits the most rapid flux density variations known for any extragalactic source. The presence of an annual cycle in the time scale for variability (Dennett-Thorpe & de Bruyn 2001), plus the measurement of a varying time delay between the IDV pattern arrival times at the VLA and WSRT (Dennett-Thorpe & de Bruyn 2002) establishes unequivocally that ISS is the mechanism responsible for the rapid flux density variability in this source. It is remarkable how readily the IDV can be seen in this source, even sampling more slowly than the characteristic time scale for variability. Clearly rapid variables like J1819+3845 would not have been missed in our survey.

Lightcurves for sources that vary on longer timescales which are well sampled by our observations are shown in Figure 3. Of particular note is J1159+2914 (B1156+295), a quasar at  $z = 0.729$  which has the highest RMS flux density observed in our survey at 167 mJy. This object has also been identified as a source of gamma-rays (Mukherjee et al. 1997) and is highly variable (e.g. Webb et al. 1995; Xie et al. 1994; Villata et al. 1997). VLBI observations reveal a high brightness temperature nucleus (Hirabayashi et al. 1998) and apparent superluminal jet speeds of up to  $9c$  ( $H_0 = 65 \text{ km s}^{-1} \text{ Mpc}^{-1}$ ,  $q_0 = 0.1$ ) have been claimed (Piner & Kingham 1997; Jorstad et al. 2001).

J0757+0956 is a BL Lac (Falomo & Ulrich 2000). It shows variability on two different timescales with quite rapid changes on a  $\sim 0.3$  day timescale and a slow overall rise in flux density over three days. This is perhaps indicative of scintillation of two sub-components in the source, one smaller than the other, or perhaps scintillation in a small component superimposed on slower intrinsic variability. Similar multi-timescale behavior is also seen in J0343+3622, J0453+0128 and J0800+4854. The continued monitoring from the remaining two epochs of our VLA program will help distinguish intrinsic from scintillation-induced variability through a search for changes in

timescale.

J1049+1429 is one of the more unusual variables and highlights the benefit of a 72 h observation. Very little variability is seen on the first and third days but on the second day we observe a  $\sim 10\%$  drop in flux density. This is consistent with variations on a characteristic time of about 1 day, in which the flux density on the first and third days happened to be nearly equal.

J1331+1712 also shows some evidence of variability on two different timescales. There is an overall increase in flux density seen over the three days together with what appears to be short-term variability on the timescale of about 1 day. In this case however the apparent short-term variability is due to resolution effects from a previously undetected extended  $\sim 1$  arcsec jet which contributes 15 mJy to the total flux density. This source was therefore not included in later MASIV survey observations.

Sources with intermediate variability timescales of 1 to 2 days are shown in Figure 4 and demonstrate the value of a 72 h observation in detecting slow variables. It is clear from the light-curves that variability in many such sources could have gone undetected with shorter monitoring periods of 2 days or less. J0102+5824 (B0059+581) shows variations on a timescale of  $\sim 1$  day. This source has been the subject of daily monitoring as part of the Keystone Project (Koyama, Kondo, & Kurihara 2001) and shows a clear annual cycle in its variability at 2.3 GHz (Jauncey et al. in preparation) with timescales ranging from 10 to  $> 100$  days. As expected for ISS, the variations are faster at 4.9 GHz and we expect to see similar changes in timescale over the course of our VLA observations.

J2237+4216, an object in our sample of weak sources, has a very high modulation index, displaying a doubling in flux density over 2 days. Little is known about this source at present but we are pursuing optical identification and VLBI imaging for this source and all other variables yet to be identified or imaged.

Varying on the longest detectable timescales are J0914+0245, J1818+5017 and J1821+6818 (Figure 5). They show a monotonic change in flux density and therefore only lower limits on their variability timescales can be estimated. If these slower changes over the three days are intrinsic in origin, then the implied variability brightness temperatures (Wagner & Witzel 1995) are greater than  $10^{16}$  K. This is well in excess of any scintillation brightness temperatures seen to date, and suggests that the IDV may have a scintillation, rather than intrinsic, origin. It will be of considerable importance to see if these sources exhibit an annual cycle which is the hallmark of ISS.

The above sources establish the ability of the survey to detect strong IDV, but it remains important to determine the limits to this ability. We are addressing this question through a detailed individual analysis of the 99 sources identified as variable. While the RMS variations in the light curves give a good indication of the flux density measurement errors for the full sample, the variability selection criterion based on the RMS alone cannot be applied blindly to individual sources. Our analysis found that in 14 of these 99 sources, the observed flux density changes were due to other causes than real variability: in particular, the presence of weak structure or weak, nearby



confusing sources.

#### 4.1. Source Properties and Statistics

Here we describe some general properties of the sources observed in the first epoch of the survey. A more detailed description of all variable sources will be left to future papers.

Of the 710 sources observed in the first epoch, a total of 85 sources (12%) are classified as variable by our RMS selection criterion. From Figure 1 it appears that there are more variable sources with high modulation indices in the weaker sample than the strong sample. To test this we divided the sources into strong and weak samples based on their 4.9 GHz flux density measured in our first epoch of observations. The weak sample was defined as all sources with a mean flux density less than 0.3 Jy with the remainder placed into the strong sample. We chose to use flux densities at 4.9 GHz instead of the 8.5 GHz JVAS and CLASS flux densities because intrinsic, long-term variability tends to be less at lower frequencies. We then selected a sample of high modulation index variables which we define as having a  $\text{RMS}/\text{mean} \geq 0.04$ . This level is well above the combined systematic (pointing) and sensitivity limits of our observations. A total of 13 sources had mean flux densities less than 60 mJy and were excluded from this analysis as our ability to detect 4% variability begins to be affected by the errors below this level. We found that of the 363 weak sources, 33 were highly variable while only 8 of the 320 strong sources were highly variable. To test this apparent difference in populations we constructed a simple chi-squared contingency test with a null hypothesis that all sources with a fractional variation  $\geq 0.04$  come from the same population and found that the probability this is true is less than 0.5%. Therefore we detect significantly more variables with high modulation indices in the weaker than the stronger source population.

### 5. Discussion

It is remarkable that of the 710 sources observed there are none that vary to the same degree as J1819+3845, a source whose intra-day variability was discovered serendipitously, and whose variability is caused by enhanced scattering within 20-40 pc of the Earth (Dennett-Thorpe & de Bruyn 2000).

Of the ten sources in Table 1 that already have optical spectroscopy, five are BL Lac objects and five are quasars. Such a high fraction of BL Lacs among the scintillators is in general agreement with the optical identification content of existing surveys (Quirrenbach et al. 2000; Kedziora-Chudczer et al. 2001).

We find there are more highly variable sources in the weaker part of our sample. There are at least two possible explanations for this. Firstly, as stated earlier, the micro-arcsecond scintillating components may simply be brightness temperature limited, in which case the weaker sources may

simply be smaller and hence are more likely to scintillate than the stronger sources. Alternatively, this effect may be the result of sampling different source populations where weaker sources are more “core dominated”, or rather less milli-arcsecond “jet dominated”. To help distinguish between these two possibilities we are imaging the 55 weakest scintillating sources with the VLBA to determine their morphology and place limits on their brightness temperatures. Follow-up observations one year later will determine the fraction of these sources that show proper motions.

We have calculated the scintillation index from a simple model based on weak scintillation theory using the Taylor and Cordes (1993) [TC93] model for the interstellar electron density and a brightness-limited model for each source. We tested two source models, in which half of the total flux density is in a Gaussian component with peak brightness of  $10^{11}\text{K}$  or  $10^{12}\text{K}$ , with the remaining flux density in regions too large to scintillate ( $> 0.1$  mas). For the  $10^{11}\text{K}$  model the predicted scintillation indices were barely detectable ( $\lesssim 0.02$ ), but for  $10^{12}\text{K}$  they were in the range 0.02 - 0.25 and are similar to those seen in our scintillators. From this we tentatively conclude that the 85 scintillators have peak brightnesses in the neighborhood of  $10^{12}\text{K}$  and the remaining sources have most of their flux density from brightness temperatures  $\lesssim 10^{11}\text{K}$ . Any decrease in the scattering distance below the 500 pc typical of the TC93 model reduces the implied brightness. Values above  $10^{12}\text{K}$  are only possible from sources with less than half of their flux density in the compact component. This brightness temperature limit is similar to those obtained from VLBI observations even though ISS is not subject to the same angular resolution limits.

The remaining epochs of our initial survey have now been observed. In future papers we will present a complete catalog of variable sources and a detailed examination of their properties. These investigations will include a comparison of changes in variability timescale with those expected due to the changing velocity of the earth relative to the LSR. Those sources that do not show these expected ISM-induced changes will be of particular interest as they may be revealing peculiar screen velocities, intrinsic flux density variability or changes in source structure that induce episodic variability.

It would seem that the boundary between intrinsic and scintillation-induced variability is not yet fully explored as demonstrated by our detection of sources that change on timescales greater than  $\sim 3$  days. For these sources it may be necessary to conduct daily observations over the course of at least a year to determine if annual cycles exist.

We are already undertaking follow-up observations of the newly detected IDVs including more intensive monitoring of the rapid variable sources with WSRT and VLBI snapshot imaging of the IDVs with previously unknown milliarcsecond-scale structures. We are also undertaking low-frequency VLBI observations of some of the brighter IDVs to search for evidence of scatter-broadening which will provide additional constraints on the size of the scattering disk.

With only a limited amount of VLBI data currently available on the variable sources it is not yet possible to draw conclusions or identify obvious trends on the relationship between milliarcsecond and microarcsecond-scale structures. The new VLBI observations we are undertaking will allow us

to address this issue.

Several of the new IDVs are regularly observed as part of geodesy and astrometry programs and some may be target phase reference sources for programs such as VERA (Honma, Kawaguchi, & Sasao 2000). A number of the weak scintillators may be amongst the most compact sources to be found at VLBI resolution and hence may form part of the astrometric radio reference frame in the future. It is important to understand the impact of scintillation. As the scintillating component in the source changes intensity as seen by a VLBI array, the observed phase center of the source will also move on the sky. The amount of movement will depend on the location and flux density contribution of the scintillating component with respect to the rest of the source.

We are extremely grateful for the technical support provided by NRAO staff at Socorro, in particular we would like to thank Ken Sowinski, Miller Goss, Mark Claussen and Jim Ulvestad. We would also like to thank Neal Jackson for providing the catalog of CLASS sources from which part of our sample was drawn. The National Radio Astronomy Observatory is a facility of the National Science Foundation operated under cooperative agreement by Associated Universities, Inc. HEB acknowledges the support of a Faculty of Science Scholarship from the University of Adelaide. BJR thanks the US-NSF for funding under grant AST 9988398.

## REFERENCES

- Aldcroft, T. L., Bechtold, J., & Elvis, M. 1994, *ApJS*, 93, 1
- Beasley, A. J., Gordon, D., Peck, A. B., Petrov, L., MacMillan, D. S., Fomalont, E. B., & Ma, C. 2002, *ApJS*, 141, 13
- Bignall, H. E. 2003, PhD Thesis, University of Adelaide.
- Bignall, H. E., Jauncey, D. L., Lovell, J. E. J., Tzioumis, A. K., Kedziora-Chudczer, L., Macquart, J-P., Tingay, S. J., Rayner, D. P., & Clay, R. W. 2003 *ApJ*, 585, 653
- Blandford, R. D. & Konigl, A. 1979, *ApJ*, 232, 34
- Brinkmann, W., Laurent-Muehleisen, S. A., Voges, W., Siebert, J., Becker, R. H., Brotherton, M. S., White, R. L., & Gregg, M. D. 2000, *A&A*, 356, 445
- Browne, I. W. A., Wilkinson, P. N., Patnaik, A. R., & Wrobel, J. M. 1998, *MNRAS*, 293, 257.
- Dennett-Thorpe, J. & de Bruyn, A. G. 2000, *ApJ*, 529, L65
- Dennett-Thorpe, J. & de Bruyn, A.G. 2001, *Astrophys. & Space Sci.*, 278, 101
- Dennett-Thorpe, J. & de Bruyn, A.G. 2002, *Nature*, 415, 57

- Drinkwater, M. J. et al. 1997, MNRAS, 284, 85
- Falco, E. E., Kochanek, C. S., & Munoz, J. A. 1998, ApJ, 494, 47
- Falomo, R. & Ulrich, M.-H. 2000, A&A, 357, 91
- Fuhrmann, L., Krichbaum, T. P., Cim, G., Beckert, T., Kraus, A., Witzel, A., Zensus, J. A., Qian, S. J., & Rickett, B. J. 2002, PASA, 19, 64.
- Heeschen, D.S. 1984, AJ, 89, 1111
- Hirabayashi, H. et al. 1998, Science, Vol. 281, Iss. 5384, p. 1825 (1998), 281, 1825
- Honma, M., Kawaguchi, N., & Sasao, T. 2000, Proc. SPIE, 4015, 624
- Jauncey, D.L., Kedziora-Chudczer, L., Lovell, J.E.J., Nicolson, G.D., Perley, R.A., Reynolds, J.E., Tzioumis, A.K. & Wieringa, M.H. 2000, , in *Astrophysical Phenomena Revealed by Space VLBI*, ed H. Hirabayashi, P.G. Edwards & D.W. Murphy, 147
- Jauncey, D. L., Bignall, H. E., Lovell, J. E. J., Kedziora-Chudczer, L., Tzioumis, A. K., Macquart, J-P., and Rickett, B. J., *Radio Astronomy at the Fringe, 2003*, Eds: J. Anton Zensus, Marshall H. Cohen, and Eduardo Ros, *Astronomical Society of the Pacific Conference Series*, 300, 199.
- Jauncey, D.L. & Macquart, J.-P. 2001, A&A, 370, L9
- Jorstad, S. G., Marscher, A. P., Mattox, J. R., Wehrle, A. E., Bloom, S. D., & Yurchenko, A. V. 2001, ApJS, 134, 181
- Kedziora-Chudczer, L., Jauncey, D.L., Wieringa, M.H., Walker, M.A., Nicolson, G.D., Reynolds, J.E., & Tzioumis, A.K. 1997, ApJ, 490, L9
- Kedziora-Chudczer, L., Jauncey, D.L., Wieringa, M.H., Tzioumis, A.K., & Reynolds, J.E. 2001, MNRAS, 325, 1411
- Kellermann, K. I., Vermeulen, R. C., Zensus, J. A., & Cohen, M. H., *Astrophysical Phenomena Revealed by Space VLBI*, *Proceedings of the VSOP Symposium*, held at the Institute of Space and Astronautical Science, Sagamihara, Kanagawa, Japan, January 19 - 21, 2000, Eds.: H. Hirabayashi, P.G. Edwards, and D.W. Murphy, Published by the Institute of Space and Astronautical Science, 159.
- Koyama, Y., Kondo, T., & Kurihara, N. 2001, Radio Science, 36, 223.
- Lähteenmäki, A. & Valtaoja, E. 1999, ApJ, 521, 493
- Macquart, J.-P., Kedziora-Chudczer, L., Rayner, D.P., & Jauncey, D.L. 2000, ApJ, 538, 623

- Marscher, A. P., Marchenko-Jorstad, S. G., Mattox, J. R., Wehrle, A. E., & Aller, M. F., In *Astrophysical Phenomena Revealed by Space VLBI*, Proceedings of the VSOP Symposium, held at the Institute of Space and Astronautical Science, Sagami-hara, Kanagawa, Japan, January 19 - 21, 2000, Eds.: H. Hirabayashi, P.G. Edwards, and D.W. Murphy, Published by the Institute of Space and Astronautical Science, 39-46.
- Mukherjee, R. et al. 1997, *ApJ*, 490, 116
- Myers, S. T. et al. 1995, *ApJ*, 447, L5.
- Narayan, R. 1992, *Phil. Trans. R. Soc. London A*, 341, 151
- Nass, P., Bade, N., Kollgaard, R. I., Laurent-Muehleisen, S. A., Reimers, D., & Voges, W. 1996, *A&A*, 309, 419
- Patnaik, A. R., Browne, I. W. A., Wilkinson, P. N., & Wrobel, J. M. 1992, *MNRAS*, 254, 655.
- Perlman, E. S., Padovani, P., Giommi, P., Sambruna, R., Jones, L. R., Tzioumis, A., & Reynolds, J. 1998, *AJ*, 115, 1253
- Piner, B. G. & Kingham, K. A. 1997, *ApJ*, 485, L61
- Quirrenbach, A., Witzel, A., Krichbaum, T., Hummel, C. A., & Alberdi, A. 1989, *Nature*, 337, 442.
- Quirrenbach, A. et al. 2000, *A&AS*, 141, 221.
- Readhead, A.C.S. 1994, *ApJ*, 426, 51
- Rickett, B.J., Quirrenbach, A., Wegner, R., Krichbaum, T. P., & Witzel, A. 1995, *A&A*, 293, 479
- Rickett, B. J., Witzel, A., Kraus, A., Krichbaum, T. P., & Qian, S. J. 2001, *ApJ*, 550, L11.
- Rickett, B. 2002, *Publications of the Astronomical Society of Australia*, 19, 100
- Rickett, B.J., Kedziora-Chudczer, L., & Jauncey, D.L., *ApJ*, 581, 103
- Taylor, J. H. & Cordes, J. M. 1993, *ApJ*, 411, 674.
- Vermeulen, R. C. & Taylor, G. B. 1995, *AJ*, 109, 1983
- Villata, M. et al. 1997, *A&AS*, 121, 119
- Wagner, S. J. & Witzel, A. 1995, *ARA&A*, 33, 163
- Walker, M. A. 1998, *MNRAS*, 294, 307.
- Webb, J. R., Barnello, T., Robson, I., & Hartman, R. C. 1995, *IAU Circ.*, 6168, 1
- Wilkinson, P. N., Browne, I. W. A., Patnaik, A. R., Wrobel, J. M., & Sorathia, B. 1998, *MNRAS*, 300, 790.

Xie, G. Z., Li, K. H., Zhang, Y. H., Liu, F. K., Fan, J. H., & Wang, J. C. 1994, A&AS, 106, 361  
Space Geodynamics Program, Huang Chen & Qian Zhihan Eds., 81.

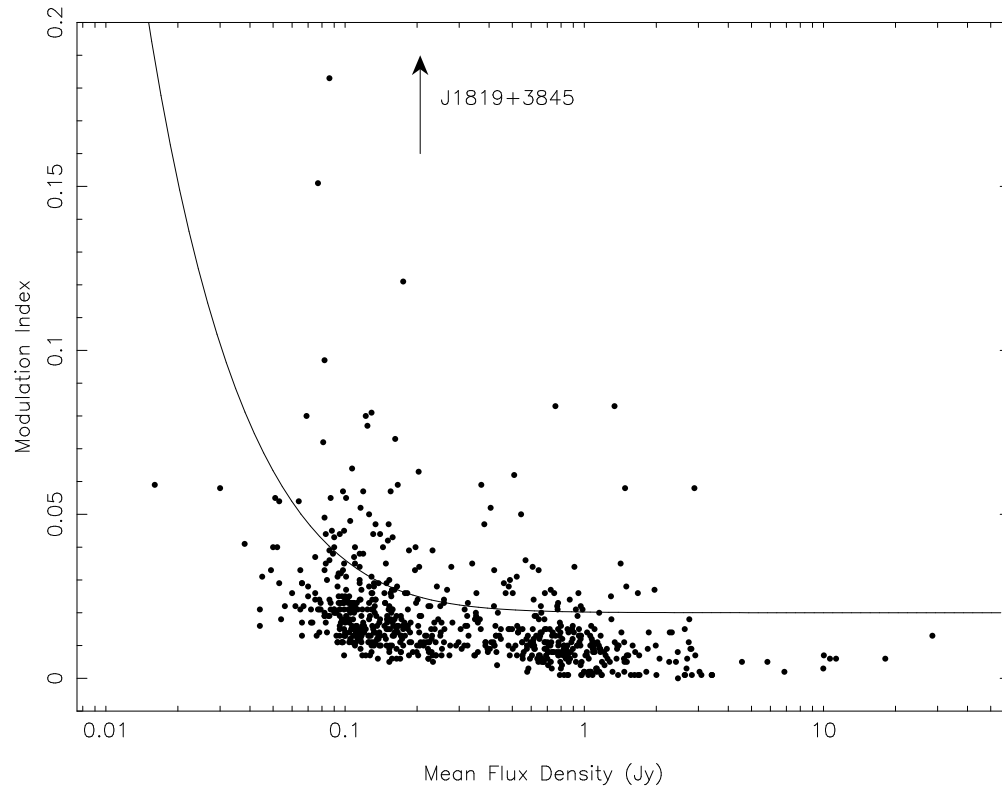


Fig. 1.— Variability index ( $\text{rms}/\bar{S}$ ) as a function of mean flux density. We classify any source above the solid line, as defined in Section 4, as variable.

Table 1. Variable sources detected in the first epoch of MASIV survey observations with mean 4.9 GHz flux density greater than 100 mJy and modulation indices of 0.04 or more.

J2000 Name	B1950 Name	$\bar{S}_{4.9}$ (Jy)	$100\sigma/\bar{S}_{4.9}$	ID	$z$	Ref
JVAS J0102+5824	B0059+581	1.34	8.3	...	...	...
CLASS J0150+2646	B0147+2631	0.12	7.7	...	...	...
JVAS J0343+3622	B0340+3612	0.76	8.3	Q	1.484	1
JVAS J0411+0843	B0408+0835	0.13	4.7	...	...	...
JVAS J0453+0128	B0450+0123	0.17	5.9	...	...	...
JVAS J0502+1338	B0459+135	0.54	5.0	BL	...	2
JVAS J0625+4440	B0621+4441	0.20	6.3	BL	...	1
JVAS J0642+8811	B0604+8813	0.20	4.0	...	...	...
JVAS J0720+4737	B0716+4743	0.37	5.9	...	...	...
JVAS J0757+0956	B0754+100	1.48	5.8	BL	...	3
CLASS J0800+4854	B0756+4902	0.11	4.0	...	...	...
JVAS J0914+0245	B0912+029	0.41	5.2	Q	0.427	4
CLASS J0916+0242	B0914+0255	0.12	5.7	...	...	...
JVAS J0929+5013	B0925+5026	0.51	6.2	BL	...	5
CLASS J0946+5020	B0942+5034	0.13	8.1	...	...	...
CLASS J1024+2332	B1022+2347	0.16	5.7	BL	...	6
CLASS J1049+1429	B1047+1445	0.16	4.3	...	...	...
JVAS J1159+2914	B1156+295	2.89	5.8	Q	0.729	7
CLASS J1328+6221	B1326+6237	0.13	5.0	...	...	...
CLASS J1331+1712	B1329+1727	0.10	5.5	...	...	...
JVAS J1610+7809	B1612+7817	0.12	5.2	...	...	...
JVAS J1656+5321	B1655+5326	0.14	4.4	Q	1.553	8
JVAS J1722+6105	B1722+6108	0.11	6.4	...	...	...
CLASS J1818+5017	B1817+5015	0.15	4.2	...	...	...
CLASS J1819+3845	B1817+3843	0.21	37.5	Q	0.54	9
JVAS J1821+6818	B1822+6817	0.13	4.4	...	...	...
CLASS J1931+4743	B1929+4737	0.11	4.8	...	...	...
CLASS J2237+4216	B2234+4201	0.18	12.1	...	...	...
CLASS J2242+2955	B2239+2939	0.15	4.7	...	...	...

Note. — Identifications (Q = quasar, BL = Bl Lac) and redshifts are given where available. Reference are (1) Vermeulen & Taylor (1995); (2) Perlman et al. (1998); (3) Falomo & Ulrich (2000); (4) Drinkwater et al. (1997); (5) Nass et al. (1996); (6) Brinkmann et al. (2000); (7) Aldcroft, Bechtold, & Elvis (1994); (8) Falco, Kochanek, & Munoz (1998); (9) Dennett-Thorpe & de Bruyn (2000)

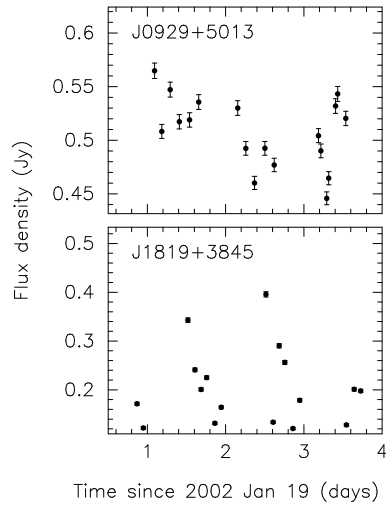


Fig. 2.— Lightcurves for two of the most rapid variables found in the survey: J0929+5013 and the previously known IDV J1819+3845.



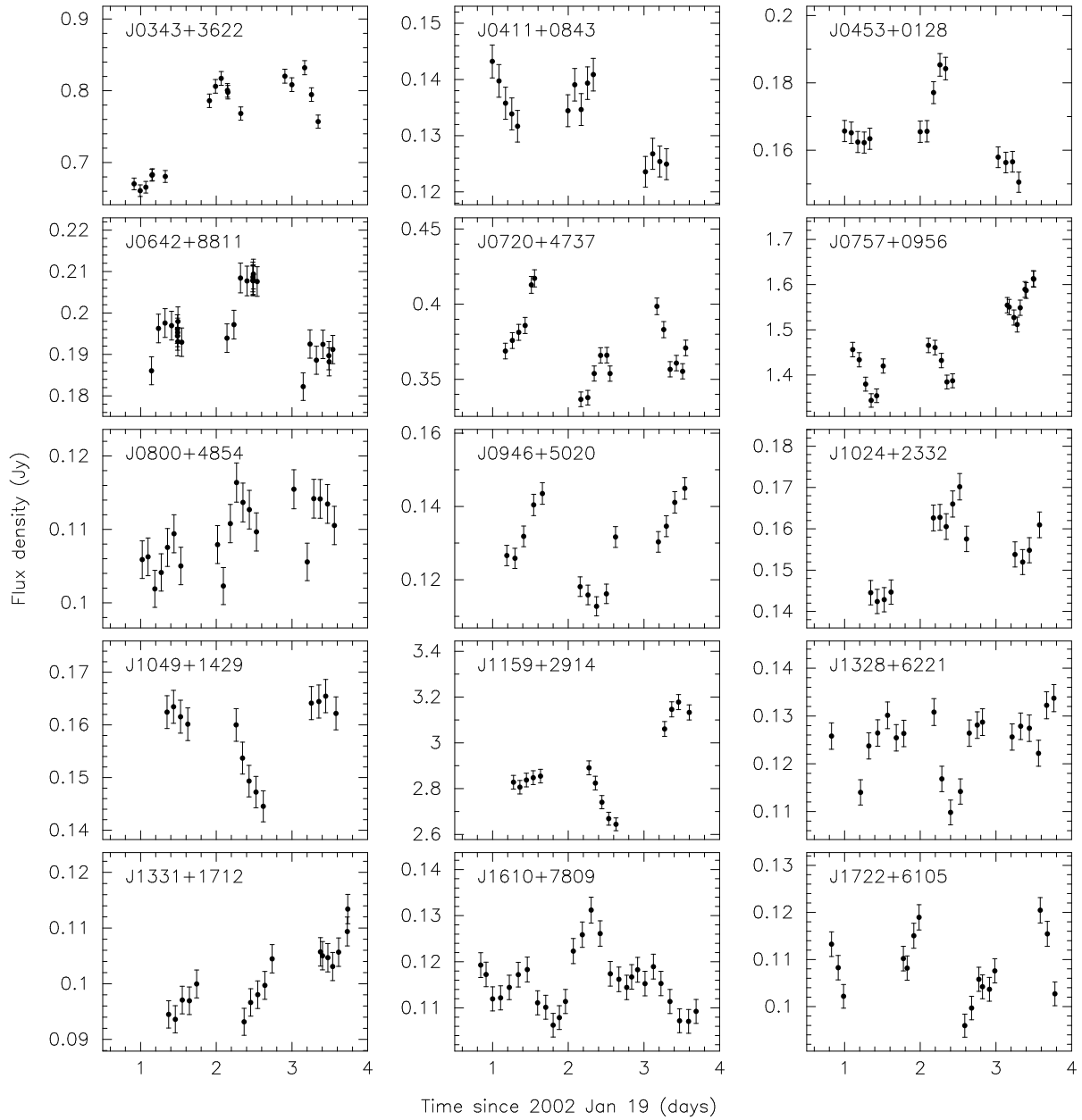


Fig. 3.— Lightcurves of variable sources with timescales ranging from a few hours to approximately one day.

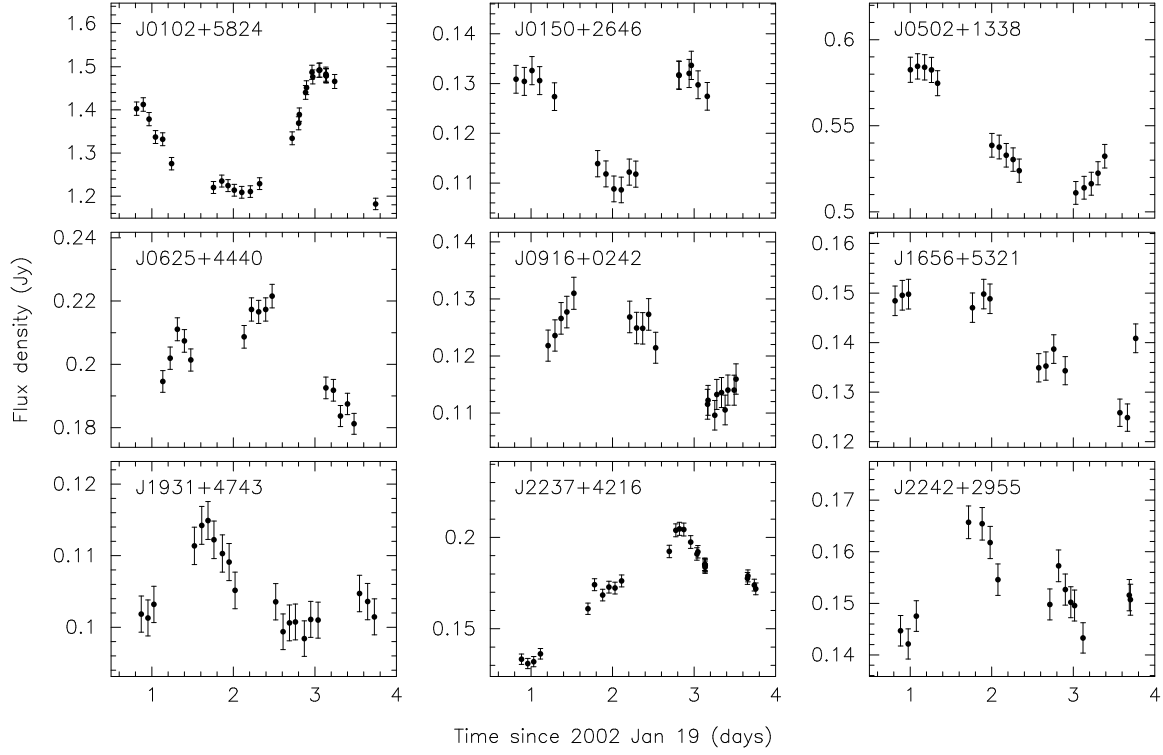


Fig. 4.— Lightcurves of sources varying on timescales of  $\sim 1$  to  $\sim 2$  days.

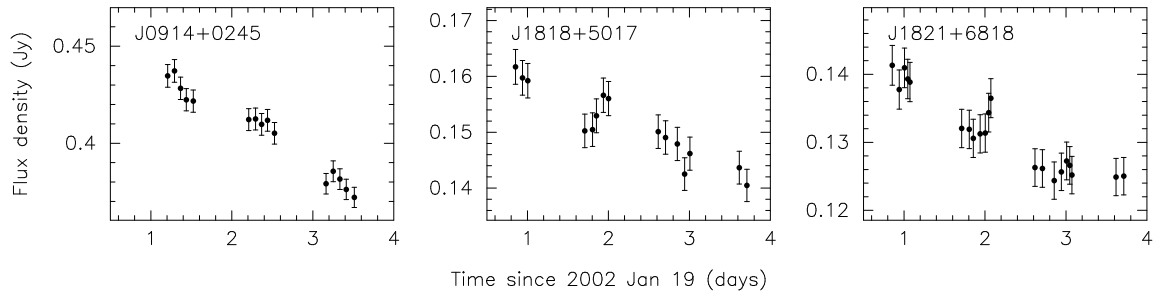


Fig. 5.— Lightcurves of sources varying on timescales longer than the period of the observations.